Proceedings of the 17th World Congress
The International Federation of Automatic Control
Seoul, Korea, July 6-11, 2008

Stability Analysis of an Electric Parking Brake (EPB) System with a Nonlinear Proportional Controller

Young O. Lee *, Choong W. Lee *, Chung C. Chung **†, Youngsup Son *, Paljoo Yoon *** and Inyong Hwang*****

**Division of Electrical and Computer Engineering, Hanyang University, Seoul, 133-791, Korea (e-mail: foryou5252@hotmail.com, chungwoo.lee@gmail.com)*
***Division of Electrical and Biomedical Engineering, Hanyang University, Seoul, 133-791, Korea (e-mail: cchung@hanyang.ac.kr)*
**** Central R&D Center, MANDO Corporation, Kyonggi-Do, 446-901, Korea (e-mail: ysson@mando.com, pjyoon@mando.com, iyhwang@mando.com)*

Abstract: In this paper, an Electric Parking Brake (EPB) system is modelled as a state-dependent switched system. The model involves screw friction which varies depending on the operation region. A new nonlinear proportional (P) controller is proposed and its stability is analyzed via Lyapunov and LaSalle's theory. It is shown that the equilibrium point is locally uniform and ultimately bounded.

1. INTRODUCTION

An Electric Parking Brake (EPB) system is a kind of X-by-wire system. The system replaces the manual maneuvering force of the conventional lever parking system with motor torque. One performance requirement is that the EPB system maintains brake force without a power supply. To satisfy this condition, the system needs to use the friction of the screw, which changes according to the operation region.

The controller of the EPB system should be designed to be robust and to provide uniform performance. First, it requires a wide range of operation due to the various weights of cars and the inclinations of roads. Second, it must tolerate large disturbance forces acting upon the parking cable due to friction on gears and screws as the pressure on the parking brake pads increases. For the EPB controller, on-off, linear proportional (P) and nonlinear P controllers were compared (Lee, *et al*., 2007). The nonlinear P controller provides good uniformity in performance and robustness.

As the EPB system's operation state varies, the screw's friction also varies. An EPB system can be modelled as a state-dependent switched system with five operation regions. It is an input-affine nonlinear system which can be approximated as a linear time-invariant system within each operation region. The nonlinear P controller has a linear gain for small error and an exponential gain about the motor's angle error for large error. Similar nonlinear PID control algorithms have been applied to a class of truck ABS problems (Jiang and Gao, 2001).

The stability of the nonlinear P controller has not been reported yet. For a switching system, stability can be shown if its individual systems share a common Lyapunov function with a negative derivative of the Lyapunov function with respect to time (Narendra and Balakrishnan, 1994). To prove the stability of the switched EPB system with the proposed nonlinear P controller, a common Lyapunov function is constructed. Because of friction, there is a self-locking state. It can be proved that the equilibrium point is locally uniform and ultimately bounded using LaSalle's theorem.

This paper is organized as follows. In Section 2, structure and characteristics of the EPB system are presented. A state-dependent switched system model is proposed. Section 3 describes the controller's specifications and its nonlinear P controller design is introduced. In Section 4, the stability analysis of the EPB system is presented. Section 5 demonstrates the performance of the controllers by experiment.

2. EPB SYSTEM MODEL

2.1 EPB System Structure and Characteristics.

The EPB is a system which controls the brake force by pulling the parking cable as in conventional existing parking brakes. The structure of the EPB system is shown in Fig. 1. It includes a DC motor, a gearbox, a screw, a nut, a current sensor, a Hall-effect force sensor, an acceleration sensor and an ECU.

Generally, if a driver or a high level system operates the EPB system, the controller calculates a target force from the parking cable based on the car mass as well as the inclination of the road as measured by the acceleration sensor. The EPB increases the brake force by pulling the parking cable using the DC motor until the brake force reaches the target force. Brake force is measured by the Hall-effect force sensor.

The EPB system has to maintain the brake force without power. To satisfy this requirement, it needs to use the friction of the screw. The direction and value of the friction may vary as the screw's rotational direction is changed. The state of the screw's friction determines the condition of the self-locking screw.

†*Corresponding author*. e-mail: cchung@hanyang.ac.kr

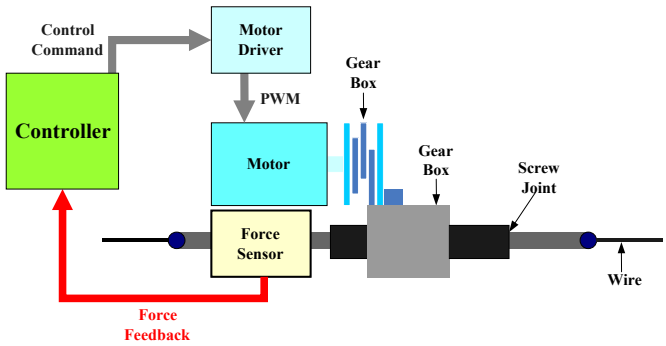

Fig. 1. Structure of the EPB system

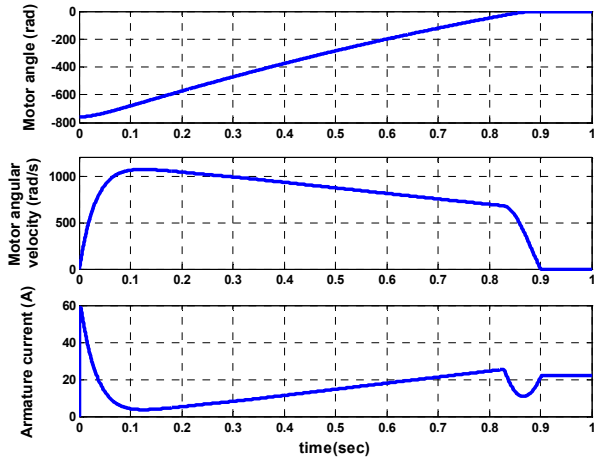

Fig. 2. Motor angle, angular velocity and armature current states. (Applying brake force mode)

Table 1. Sign of the state variables

State variable	Apply	Release
Motor angle	$\theta \le 0$	$\theta \ge 0$
Motor angular velocity	$\dot{\theta} \ge 0$	$\dot{\theta} \le 0$
Armature current	$i \ge 0$	$i \le 0$

Fig. 2 shows typical simulation results for the EPB system with a nonlinear P controller which will be discussed in section 3. As the angular velocity approaches zero, the armature current demonstrates the Stribeck effect. Once the screw is self-locked, the angular velocity and the armature current are maintained due to screw friction. Table 1 shows signs of the states at each operation mode. Notice that the product of the motor angle and the armature current is always negative semi-definite regardless of the operation mode.

2.2 State Dependent Switched Model of EPB

The EPB system is a highly nonlinear system due to friction. The friction of the screw varies depending on the operation region. Therefore, the EPB system can be modelled as a state-dependent switched system. The general friction model can be described as in (1) (Olsson, et al., 1998). F_e describes the external force. The maximum static friction force F_s is assumed to be larger than zero.

$$F_r(v, F_e) = \begin{cases} F(v) & if\ v \neq 0 \\ F_e & if\ v = 0\ \ and\ |F_e| < F_s \\ F_s \operatorname{sgn}(F_e) & if\ v = 0\ \ and\ |F_e| \geq F_s \end{cases} \quad (1)$$

When the velocity, v, is not zero, the friction model includes the Coulomb friction F_c, the maximum static friction F_s, the coefficient of viscous friction F_v and the Stribeck friction with Stribeck velocity v_s.

$$F(v) = F_c + (F_s - F_c)e^{-|v/v_s|^{\delta_s}} + F_v v \quad (2)$$

The screw of the EPB system has a lower magnitude of viscous and Stribeck friction than static friction and Coulomb friction in the range of interest. The friction model can be simplified for stability analysis as follows:

$$F_r(v, F_e) = \begin{cases} F_c & if\ v \neq 0 \\ F_e & if\ v = 0\ \ and\ |F_e| < F_s \\ F_s \operatorname{sgn}(F_e) & if\ v = 0\ \ and\ |F_e| \geq F_s \end{cases} \quad (3)$$

Here, external force F_e and Coulomb friction F_c can be described as in (4) and (5). T is the torque whose direction is perpendicular to the screw plane, Q is the force applied in the screw axial direction, d is the screw diameter, λ is the screw lead angle and μ_s is the friction coefficient of the screw.

$$F_e = \frac{2}{d} T \cos\lambda - Q \sin\lambda \quad (4)$$

$$F_c = \mu_s \left(\frac{2}{d} T \sin\lambda + Q \cos\lambda \right) \quad (5)$$

$$Q = \begin{cases} \alpha_1 T & if\ v \neq 0\ and\ F_e v > 0 \quad (6\text{-a}) \\ \alpha_2 T & if\ v \neq 0\ and\ F_e v < 0 \quad (6\text{-b}) \\ \alpha_3 T & if\ v = 0\ and\ |F_e| < F_s \quad (6\text{-c}) \\ \alpha_4 T & if\ v = 0\ and\ |F_e| \geq F_s\ and\ F_e > 0 \quad (6\text{-d}) \\ \alpha_5 T & if\ v = 0\ and\ |F_e| \geq F_s\ and\ F_e < 0 \quad (6\text{-e}) \end{cases}$$

The relation between input torque T and output force Q is modelled as linear in each screw's operation state. Each state is as follows. (6-a) and (6-b) show acceleration and deceleration modes, respectively. (6-c) is the case of the self-locking state, $\alpha_3 \equiv 0$ is maintained. (6-d) is the case where the

screw begins to rotate forward to apply force for pulling the parking cables. (6-e) is the case where the screw begins to rotate backward to release the parking cables. α_n is the screw gain corresponding to each case.

These conditions result in a state-dependent switched EPB system (7). The system is an input-affine nonlinear system.

$$\dot{x} = A(x)x + Bu \tag{7}$$

The system matrix $A(x)$ varies depending on the system switch-states and it can be redefined as in (8)

$$A(x) = A_n, \quad \forall x \in \Omega_n, \ n = 1, \cdots, 5 \tag{8}$$

where the operating region, Ω_n, is defined at each switching condition. At each Ω_n, (7) is a linear time-invariant system.

The set S consists of 5 ordered pairs, system matrices and operating regions. It can be defined as

$$S = \{(A_1, \Omega_1), \cdots, (A_5, \Omega_5)\} \tag{9}$$

where A_n and Ω_n satisfy the conditions of (10).

$$A_n \in \mathbb{R}^{3\times 3}, \ \Omega_n \in \mathbb{R}^3, \quad \bigcup_{n=1}^{5} \Omega_n = \mathbb{R}^3, \ \forall n \neq m, \ \Omega_n \cap \Omega_m = \varnothing \tag{10}$$

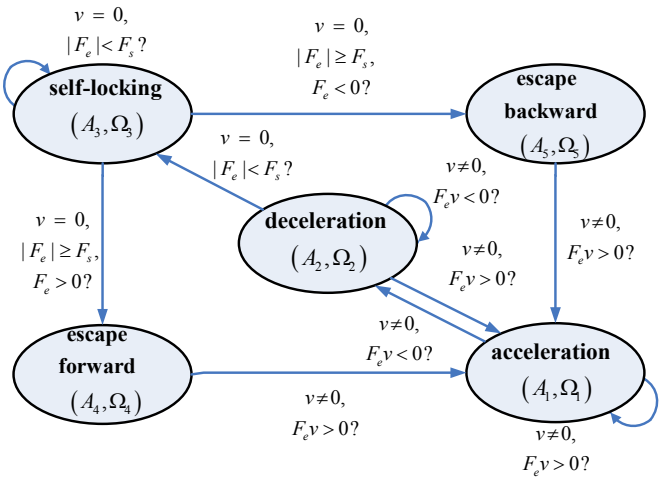

Fig. 3. State diagram of EPB system

The state switches occur in restricted directions. These relations can be described in Fig. 3. When the screw is in a self-locking state (Ω_3), if the magnitude of the external force is larger than the maximum static friction force of the screw, it begins to rotate either backward (Ω_5) or forward (Ω_4). It then accelerates (Ω_1). Generally, it maintains its acceleration state (Ω_1) for some time. After some period of time, it decelerates (Ω_2). Depending on its velocity, the deceleration state is switched to either acceleration or self-locking states.

State space equations can be classified into two groups. When a mechanical system is moving or starting to move, (11-a) is used. When a mechanical system is locked by friction, (11-b) is used. The state variables are the motor angle, θ, the motor angular velocity, ω and the armature current, i. L_a is the armature inductance, R_a is the armature resistor, J is the inertia at the armature, K_b is the back emf constant and K_t is the motor torque constant.

$$(\text{Case A}) \ n = 1, 2, 4, 5$$

$$\begin{bmatrix} \dot{\theta} \\ \dot{\omega} \\ \dot{i} \end{bmatrix} = \begin{bmatrix} 0 & 1 & 0 \\ -\frac{\beta_n}{J} & 0 & \frac{K_t}{J} \\ 0 & -\frac{K_b}{L_a} & -\frac{R_a}{L_a} \end{bmatrix} \begin{bmatrix} \theta \\ \omega \\ i \end{bmatrix} + \begin{bmatrix} 0 \\ 0 \\ \frac{1}{L_a} \end{bmatrix} V_{in} \tag{11-a}$$

$$y = \begin{bmatrix} 1 & 0 & 0 \end{bmatrix} \begin{bmatrix} \theta \\ \omega \\ i \end{bmatrix}$$

$$(\text{Case B}) \ n = 3$$

$$\begin{bmatrix} \dot{\theta} \\ \dot{\omega} \\ \dot{i} \end{bmatrix} = \begin{bmatrix} 0 & 0 & 0 \\ 0 & 0 & 0 \\ 0 & 0 & -\frac{R_a}{L_a} \end{bmatrix} \begin{bmatrix} \theta \\ \omega \\ i \end{bmatrix} + \begin{bmatrix} 0 \\ 0 \\ \frac{1}{L_a} \end{bmatrix} V_{in} \tag{11-b}$$

$$y = \begin{bmatrix} 1 & 0 & 0 \end{bmatrix} \begin{bmatrix} \theta \\ \omega \\ i \end{bmatrix}$$

In equation (11-a), variable β_n is related to the screw gain, α_n, which varies with the screw's operating condition. It models the relation between the load of the parking cable and the motor's angle as linear. C_w is the spring constant of the parking cable. C_{fs} is the spring constant of the force sensing spring. N_{GR} is the gear box's gear ratio and p is the screw pitch.

$$\beta_n = \frac{1}{N_{GR}^{\ 2}} \frac{p}{2\pi\alpha_n} \frac{C_w C_{fs}}{C_w + 2C_{fs}}, \quad n = 1, 2, 4, 5 \tag{12}$$

3. CONTROL SYSTEM DESIGN

3.1 Performance Requirement

The following performance specifications are required for the EPB system in general (Jaume, *et al.,* 2004):

-The system must brake the car without a power supply.

-The system must generate the demanded braking force within a specified time.

-The mechanical design has to be durable and robust.

-It is advisable that the EPB system be silent.

To satisfy the first specification, the EPB system uses the self-locking principle of the screw-nut structure. Therefore, it is essential to limit the direction of the controller output when applying the EPB. This limitation prevents the interrupt of the screw self-locking mechanism by reverse rotation of the motor.

The required parking cable tension is determined by the weight of the car and the inclination of the road. Because electronic components are added to the EPB system, the robustness and safety issues become more important than in conventional parking brake systems. Performance of three controllers (on-off, linear P and nonlinear P) was compared by Lee, *et al*., (2007). The nonlinear P controller shows good robustness performance compared with other control methods.

3.2 Nonlinear P Controller Design

The nonlinear P controller (13) uses the nonlinear function $f(e, K_{p\_nl}, \alpha, \delta)$. It applies high gain for small error and small gain for large error. To avoid excessive high gain and unwanted vibrating response in the neighbourhood of the equilibrium point, it uses a linear gain for small error (Jiang and Gao, 2001) as shown in Fig. 4. The output direction of the controller should be maintained in the same direction as the motor's movement to prevent the motor from rotating in reverse. In a real system, due to physical limitations, the control output is bounded. The control output is defined by

$$u = f\left(e, K_{p\_nl}, \alpha, \delta\right) \tag{13}$$

where e is the motor angle error and K_{p_nl}, α and δ are user design parameters. The nonlinear function is given by

$$f\left(e, K_{p\_nl}, \alpha, \delta\right) = \begin{cases} K_{p\_nl}\delta^{\alpha-1}e, & 0 \le |e| \le \delta \\ K_{p\_nl}|e|^{\alpha-1}e, & \delta < |e| \le r. \end{cases} \tag{14}$$

Here,

$$\forall \alpha \in (0,\ 1),\quad e = \theta_d - \theta,$$
$$K_{p\_nl} > 0,\quad \delta > 0,\quad r > 0$$

Assumption 1. Within the operation range where the control output is an exponential function of the angle error, the magnitude of the motor's angular velocity is larger than or equal to 1[rad/s]. In other words,

$$|\dot{\theta}| \ge 1 \quad [rad/s] \tag{15}$$

for $|r| \ge |e| > \delta$.

Remark 1. For our system, r is about 800[rad], δ is around 20[rad] and EPB should be locked within 1[sec]. It is clear that assumption 1 is physically reasonable and the condition in (15) is satisfied once the power is applied.

Assumption 1 is needed to satisfy the stability of this system. Details on stability will be explained in section 4.

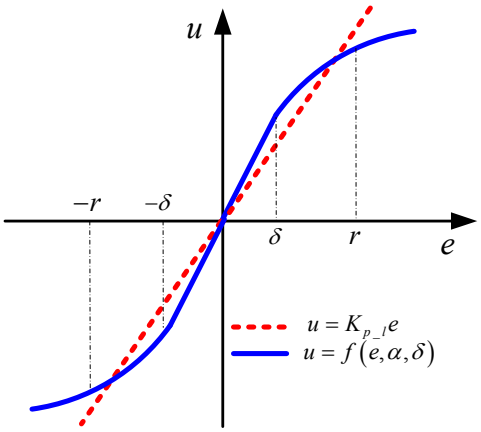

Fig. 4. The functions of the Linear P and the Nonlinear P controller.

4. STABILITY ANALYSIS

4.1 Stability of the Nonlinear P Controller EPB System

The output of the controller is a nonlinear function dependent on the state variable $x_1=\theta$. Input voltage becomes (16) and function f is described in (14). The origin of $\mathbb{R}^3$ is taken as the equilibrium point without loss of generality (Khalil, 2003).

$$V_{in} = f\left(e, K_{p\_nl}, \alpha, \delta\right) \tag{16}$$

The state-space model of the EPB system with a nonlinear controller can be described as a combination of linear and nonlinear elements described by

$$\dot{x} = \left(A_{c,n} + B(x)\right)x,\ \ \forall x \in \mathbb{R}^3 \tag{17}$$

$$A_{c,n}=\begin{bmatrix} 0 & 1 & 0 \\ -\frac{\beta_n}{J} & 0 & \frac{K_t}{J} \\ -\frac{K_{p\_nl}}{L_a}\delta^{\alpha-1} & -\frac{K_b}{L_a} & -\frac{R_a}{L_a} \end{bmatrix} \quad \text{for} \quad x\in\mathbb{R}^3/\Omega_3 \tag{18-a}$$

and

$$A_{c,n}=\begin{bmatrix} 0 & 0 & 0 \\ 0 & 0 & 0 \\ -\frac{K_{p\_nl}}{L_a}\delta^{\alpha-1} & 0 & -\frac{R_a}{L_a} \end{bmatrix} \quad \text{for} \quad x\in\Omega_3 \tag{18-b}$$

$$B(x)=\begin{cases} 0, & 0\le|e|\le\delta \\ \begin{bmatrix} 0 & 0 & 0 \\ 0 & 0 & 0 \\ \frac{K_{p\_nl}}{L_a}\left(\delta^{\alpha-1}-|e|^{\alpha-1}\right) & 0 & 0 \end{bmatrix}, & \delta<|e|\le r \end{cases} \tag{19}$$

From the root locus analysis, we can easily show that there exist $K_{p,min}$ and $K_{p,max}$, such that

$$\begin{aligned} &\sigma\left(A_{c,n}\right)\subset\mathbb{C}_-^0 \quad \text{for} \\ &K_{p\_nl}\delta^{\alpha-1}\in\left(K_{p,\min},\ K_{p,\max}\right) \\ &\forall x\in\Omega_n,\ \ n=1,\ 2,\ 4,\ 5 \end{aligned} \tag{20}$$

where $\sigma(A_{c,n})$ is the spectrum of the system matrix $A_{c,n}$. A common Lyapunov function is shown in (21)

$$V(x)=\begin{cases} x^TPx+\frac{K_{p\_nl}}{L_a}\delta^{\alpha}p_{31}x_1^2, & 0\le|e|\le\delta \\ x^TPx+\frac{1}{3}\frac{K_{p\_nl}}{L_a}\delta^{\alpha+2}p_{31} & \\ \quad+\frac{2}{3}\frac{K_{p\_nl}}{L_a}\mathrm{sgn}(x_1)\delta^{\alpha-1}p_{31}x_1^3, & \delta<|e|\le r \end{cases} \tag{21}$$

Let $p_{mn}=P(m,n)$

Assumption 2. The (3, 1), (3, 2) and (3, 3) components of the *P* matrix must be greater than zero.

$$p_{31}>0,\ p_{32}>0,\ p_{33}>0$$

Remark 2. Given the set of $A_{c,n}$, as long as we are able to find *P*, which is the solution of the common Lyapunov function, p_{31}, p_{32} and p_{33} are positive.

If $\exists\ P=P^T>0$ for some $Q_n=Q_n^T>0$ satisfying $A_{c,n}{}^TP+PA_{c,n}=-Q_n$, $\forall x\in\Omega_n$, n=1,2,4,5. Because $\mathrm{sgn}(x_1)x_1^3>0$. It is clear that *V(x)* is locally positive definite and continuously differentiable.

Then the derivative of *V(x)* is given by

$$\dot{V}(x)=\begin{cases} -x^TQ_nx & \\ \quad+2\frac{K_{p\_nl}}{L_a}\delta^{\alpha}p_{31}x_1x_2, & \forall\,0\le|e|\le\delta \\ -x^TQ_nx+2x^TB(x)^TPx & \\ \quad+2\mathrm{sgn}(x_1)\frac{K_{p\_nl}}{L_a}\delta^{\alpha-1}p_{31}x_1^2x_2, & \forall\,\delta<|e|\le r \end{cases} \quad \text{for } \forall x\in\Omega_n,\ n=1,2,4,5 \tag{22}$$

When $0\le|e|\le\delta$, it is clear that $\dot{V}(x)$ is negative definite since we have $x_1x_2\le0$ from Table 1.

When $\delta<|e|\le r$, the second term of $\dot{V}(x)$, $2x^TB(x)^TPx$, is equal to (23).

$$\begin{aligned} &2x^TB(x)^TPx \\ &=2\frac{K_{p\_nl}}{L_a}x_1\left(\delta^{\alpha-1}-|e|^{\alpha-1}\right)\left(p_{31}x_1+p_{32}x_2+p_{33}x_3\right) \end{aligned} \tag{23}$$

(23) is always negative if the $K_{p\_nl}p_{31}x_1{}^2(\delta^{\alpha-1}-|e|^{\alpha-1})/L_a$ term is eliminated as shown in (24) since $x_1x_2\le0$ and $x_1x_3\le0$ in the operation range without loss generality .

$$\begin{aligned} &2x^TB(x)^TPx-2\frac{K_{p\_nl}}{L_a}p_{31}x_1^2\left(\delta^{\alpha-1}-|e|^{\alpha-1}\right) \\ &=2\frac{K_{p\_nl}}{L_a}x_1\left(\delta^{\alpha-1}-|e|^{\alpha-1}\right)\left(p_{32}x_2+p_{33}x_3\right)\le0 \end{aligned} \tag{24}$$

We see that (25) holds, since $-\mathrm{sgn}(x_1)x_2\ge1$ from Assumption 1.

$$\begin{aligned} &2\frac{K_{p\_nl}}{L_a}p_{31}x_1^2\left(\delta^{\alpha-1}-|e|^{\alpha-1}\right) \\ &<-2\mathrm{sgn}(x_1)\frac{K_{p\_nl}}{L_a}\delta^{\alpha-1}p_{31}x_1^2x_2 \end{aligned} \tag{25}$$

From (24) and (25), we see that

$$\begin{aligned} &2x^T B(x)^T Px + 2\,\mathrm{sgn}(x_1)\frac{K_{p\_nl}}{L_a}\delta^{\alpha-1}p_{31}x_1{}^2x_2 \\ &< 2x^T B(x)^T Px - 2\frac{K_{p\_nl}}{L_a}p_{31}x_1{}^2\left(\delta^{\alpha-1} - |e|^{\alpha-1}\right) \le 0 \end{aligned} \tag{26}$$

Because $\dot{V}(x) \le -x^T Q_n x, \forall x \notin \Omega_3$, the states converge to Ω_3 exponentially.

4.2 Self-locking State Stability

In section 4.1, we showed that, if x starts in $\mathbb{R}^3/\Omega_3$, x approaches Ω_3 as $t \to \infty$. Since

$$\dot{V}(x) \le -x^T Q_n x, \forall x \notin \Omega_3 \tag{27}$$

In the self-locking state, the operating region is defined as (28) and $\dot{x}_1 = \dot{x}_2 = 0,\ \forall x \in \Omega_3$.

$$\Omega_3 = \left\{ x \mid \dot{x}_1 = \dot{x}_2 = 0, |F_e| < F_s,\ x \in \mathbb{R}^3 \right\} \tag{28}$$

We know that if $\dot{x}_1 = \dot{x}_2 = 0,\ \forall x \in \Omega_3$ then the derivative of the Lyapunov function (21) becomes

$$\begin{aligned} \dot{V}(x) &= 2\left(x_1 \dot{x}_3 p_{13} + x_3 \dot{x}_3 p_{33} \right) \\ &= -2\left(\frac{K_p}{L_a}x_1 + \frac{R_a}{L_a}x_3 \right)\left(x_1 p_{13} + x_3 p_{33} \right) \\ &= -2\left\{ \frac{K_p p_{13}}{L_a}x_1{}^2 + \frac{R_a p_{33}}{L_a}x_3{}^2 + x_1 x_3 \left(\frac{R_a p_{13}}{L_a} + \frac{K_p p_{33}}{L_a} \right) \right\} \end{aligned} \tag{29}$$

where $K_p = K_{p\_nl}\delta^{\alpha-1}$. Define the set M, such that

$$M = \left\{ x \mid K_p p_{13} x_1{}^2 + R_a p_{33} x_3{}^2 + x_1 x_3 \left(R_a p_{13} + K_p p_{33} \right) > 0 \right\} \tag{30}$$

The closure of the set M is on the x_1-x_3 plane in R^3.

Then it is clear that

$$\dot{V}(x) < 0,\ \ \forall x \in M$$

and

$$\dot{V}(x) \equiv 0,\ \forall x \in \Omega_3 \cap \partial M \cap N$$

where

$$N = \left\{ x \mid K_p x_1 + R_a x_3 = 0 \text{ or } p_{13}x_1 + p_{33}x_3 = 0 \right\} \tag{31}$$

The motor current is maintained after the screw is self-locked as in Fig. 2. So the derivative of the motor current becomes zero.

In the self-locking state, the largest invariant set becomes

$$\Omega_3 \cap \partial M \cap N \tag{32}$$

The largest invariant set is the intersection of the closure of the set M (30) and the set N (31) on the x_1-x_3 plane. Therefore, the largest invariant set becomes a set of the two intersection points.

Using LaSalle's theorem, we can show that the equilibrium point is locally uniform and ultimately bounded.

Fig. 5 shows the value of the Lyapunov function. It is positive within the operation range and its derivative with respect to time is negative.

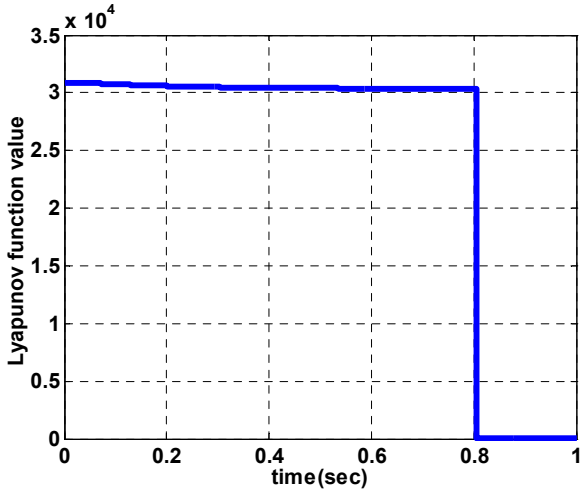

Fig. 5. Lyapunov Function Value

5. EXPERIMENTAL RESULT

Fig. 6 shows the experimental result of cable force and nonlinear control signal at each operation mode. It is controlled by a PWM method, so maximum value of control signal 100 [%]. (a) shows the cable force and (b) shows the control signal when the EPB system applies brake force. (c) and (d) show when the brake force is released. The target force of apply mode is assumed to be 980[N] and the one of release mode is assumed to be 0[N].

In the applied mode, although the control signal exists, once the state enters the self-locking region, Ω_3, the cable force is maintained due to the screw's friction. In the release mode, because the screw friction is small, the response time is faster than the applied mode. The cable force is decreased after the control signal becomes zero due to large inertia.

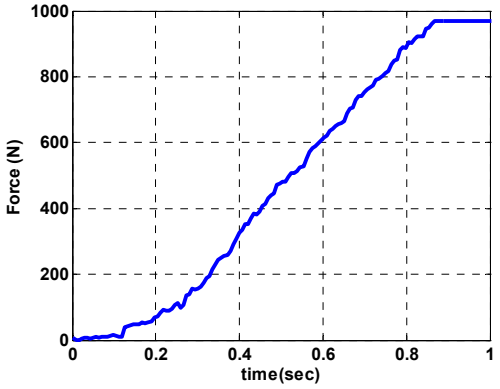

(a) Parking cable force (apply mode)

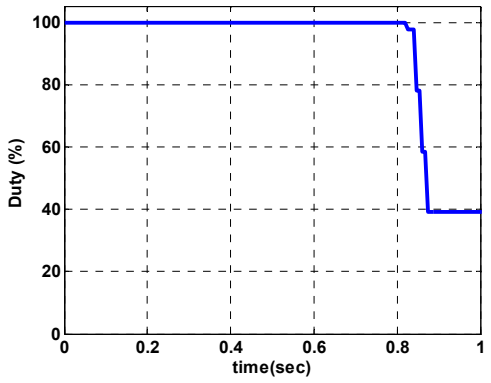

(b) Control signal (apply mode)

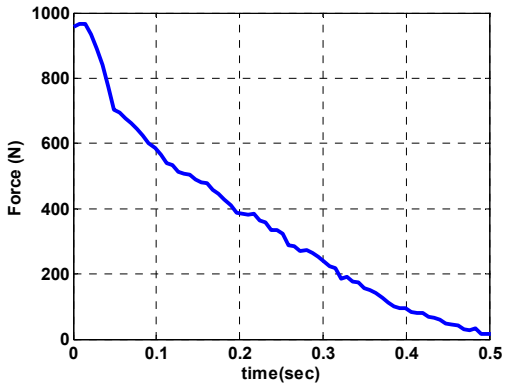

(c) Parking cable force (release mode)

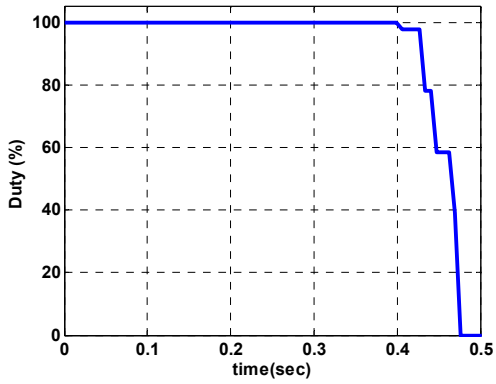

(d) Control signal (release mode)

Fig. 6. Experimental result: Target forces for (a) and (c) are 980[N] and 0[N], respectively.

6. CONCLUSIONS

This paper introduced an EPB system and described its characteristics. The EPB system was modelled as a state-dependent arbitrary switched system. The control requirements were explained and the nonlinear P controller was proposed. The stability of the closed-loop system was investigated by applying Lyapunov and LaSalle's theory. The states converge to a self-locking state exponentially and the equilibrium point is locally uniform and ultimately bounded. Through experimental results, the performance of the nonlinear P controller was shown.

ACKNOWLEDGMENT

This paper was supported in part by the Components and Materials Technology Development Program of MCIE, Republic of Korea under Grant 10014728.

This work was supported by the Brain Korea 21 Project in 2007.

REFERENCES

Jaume, P., J. Jordi, Dr. A. Jesus, Dr. C. Ismael and F. Sergi (2004). Conceptions of actuators for an electric parking brake (EPB). *FISITA technical paper,* Document No. F2004F182.

Jiang, F. and Z. Gao (2001). An Application of Nonlinear PID Control to a Class of Truck ABS Problems. *Proceedings of IEEE Conf. on Decisions and Control,* **1**, pp. 516-521.

Khalil, Hassan K (2002). *NONLINEAR SYSTEM (3rd edition),* pp. 112, Prentice Hall.

Lee, Y.O., C. W. Lee, H.B. Chung, C. C. Chung, Y. Son, P. Yoon and I. Hwang (2007). A Nonlinear Proportional Controller for Electric Parking Brake (EPB) Systems. *14th Asia Pacific Automotive Engineering Conference,* Document No. 2007-01-3657.

Narendra, K.S. and J. Balakrishnan, (1994). A Common Lyapunov Function for Stable LTI Systems with Commuting A-Matrices. *IEEE Transactions on automatic control,* **39**(12), pp. 2469-2471.

Olsson, H., K. J. Åström, C. C. de Wit, M. Gäfvert and P. Lischinsky (1998). Friction models and friction compensation. *European Journal of Control,* **4**, pp. 176-195.